

average 6 times higher than from 3DCT scans of the same length. This is due to the much lower pitch used for 4DCT scans and the auto mA option is not available for 4DCT scanning.

Our results have shown that the proposed strategy of acquiring a FL-3D scan in conjunction with a RL-4DCT scan reduces the dose to about 4 times that received from a FL-3D scan.

The values quoted by Matsuzaki et al. (2013), are about 1.5 to 2 times lower than those obtained in this study although the same scanner was used in both studies. The reason for this is that they used lower mAs and higher pitch. Therefore, this indicates that there may be potential for further imaging dose reduction through optimizing mAs values for 4DCT acquisition in our institution.

PO-0957

Improved automatic bone segmentation in pelvis using a customized excitation pulse on MR

M. Maspero¹, P.R. Seevinck², A. Andreychenko¹, S. Crijns¹, A. Sbrizzi³, M. Viergever², J.W. Lagendijk¹, C.A.T. Van Den Berg¹
¹UMC Utrecht, Department of Radiation Oncology, Utrecht, The Netherlands

²UMC Utrecht, Image Sciences Institutes, Utrecht, The Netherlands

³UMC Utrecht, Department of Radiology, Utrecht, The Netherlands

Purpose/Objective: Recently, the pseudo-CT generation based on Dixon water/fat imaging sequences has been proposed ([1] Schadewaldt et al. IJROBP 2013). Although promising, a remaining challenge of the methodology is the misclassification of air/liquid mixtures to bone. These mixtures are characterized by short T_2^* , albeit much longer than T_2^* of cortical bone, leading to signal voids at regular 1.5 T water and fat in-phase echo times (T_E). The aim of this study is to reduce the misclassification of bone in order to obtain more reliable depiction of the bony anatomy on Digitally Reconstructed Radiography (DRR) useful in patient positioning.

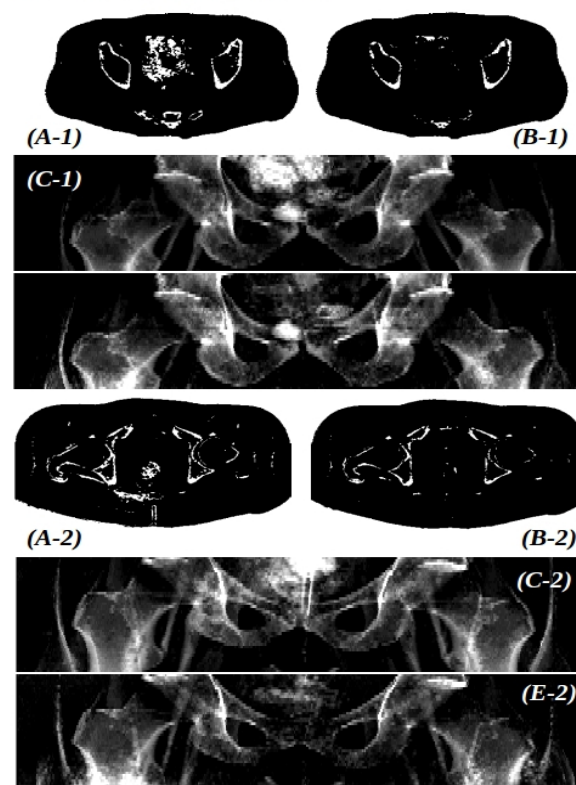
Materials and Methods: Two healthy volunteers were subjected to MRI scanning on a 1.5 T system in accordance with the IRB guidelines. The scanner software was modified to allow the use of a custom designed spectral-spatial selective excitation RF pulse.

Whereas a conventional excitation pulse does not influence the relative phase of water and fat, leading to a first water/fat In-Phase (IP) T_E of 4.6 ms at 1.5 T, the proposed pulse was designed in such a way that the water/fat IP (or Out-of-Phase (OP)) T_E can be freely chosen.

IP and OP images ('Pulse' in the Fig.) were obtained in two separated acquisitions with $T_E/T_R = 2.3/5.3$ ms by designing two dedicated RF pulses. The two pulses did not need to be designed repeatedly for different subjects. Two conventional IP and OP images ('Reference' in the Fig.) were also acquired with T_E equal to 2.3 and 4.6 ms ($T_R = 3.6$ and 5.8 ms), respectively similar to [1]. The four scans (3D cartesian spoiled gradient echo, matrix 43x132x200, FOV 12.9x26.4x40 cm³, $\alpha = 7^\circ$) were acquired consecutively within a 100 s time period to minimize the probability of varying bowel filling in between scans.

Body contour segmentations were obtained using an automatic 3 classes threshold Otsu algorithm on the IP images. Segmentation of bone anatomy in the form of binary masks (A,B) was generated applying a 3 classes k-mean clustering algorithm on the IP and OP images. Bone-only DRRs were reconstructed from the bone segmentations (C,D).

Body and bone masks of the same transverse slice for the reference (A) and pulse (B) image. Bone-only DRR from the Reference (C) and the Pulse (D) images. The data of both of the volunteers (1,2) are presented.



Results: The use of the custom designed pulse in combination with a novel image processing approach leads to less T_2^* signal dephasing as the IP T_E could be reduced from 4.6 to 2.3 ms. As a result, we have less misclassification of bone allowing the generation of DRR with reduced artifact level. Some false positives in the bowel region still remained in the segmentation but no additional image processing was applied in order to stress the actual contribution of the pulse. This could be addressed by image processing techniques similar as in [1].

Conclusions: We showed that the use of a custom designed excitation pulse in combination with the proposed image processing method allows the creation of an IP echo at earlier time minimizing T_2^* decay and there misclassification in the bowel region. This enables comparable or better than conventional segmentation of bone anatomy in the pelvis.

Future work will focus on a further reduction of bone misclassification and on the development of a multi-echo MR acquisition protocol in order to obtain IP and OP images in a single sequence.

PO-0958

Correlations between DCE-MRI, [18F]-FLT PET and survival in patients with high grade glioma

P. Brynolfsson¹, T. Asklund², M. Gref³, J. Axelsson⁴, K. Riklund⁵, T. Nyholm¹

¹Umeå University, Department of Radiation Sciences, Umeå, Sweden

²Umeå University, Department of Radiation Sciences and Oncology, Umeå, Sweden

³Umeå University Hospital, Department of Radiology, Umeå, Sweden

⁴Umeå University Hospital, Radiation Sciences, Umeå, Sweden

⁵Umeå University Hospital, Department of Radiation Sciences, Umeå, Sweden

Purpose/Objective: DCE-MRI and FLT PET have been reported to predict treatment response in several diagnoses and treatment regimes. In this pilot study we investigate correlations between model-based and non-model based parameters from DCE-MRI analysis and the maximum standardized uptake value (SUV(max)) in the tumor; and their correlations to survival.

Materials and Methods: Eight patients undergoing first line treatment (conformal radiotherapy 2/60 Gy, concomitant with temozolamide) for high grade glioma were included in the study. PET and MRI imaging were done within one week of treatment start and at two weeks into treatment. All PET images were acquired using a GE Discovery 690 scanner and reconstructed using Sharp IR with 3 iterations and 24 subsets. All MRI images were acquired using a 1.5 T Siemens Espree with a 12-channel head coil. The DCE-MRI analysis was performed on in-house software using the Tofts model to calculate Ktrans, with an arterial input function generated with the Parker model. A non-model-based parameter, initial area under the gadolinium curve of the first 60 seconds of after bolus arrival (IAUGC60) was also calculated. Regions of interest (ROIs) were delineated on contrast-enhanced T1-weighted images by an oncologist, and mean, min, max and standard deviation (SD) was calculated within each ROI for Ktrans and IAUGC60. SUV(max) was identified in the tumor region for each patient. Example SUV, IAUGC60 and Ktrans parameter maps are shown in Figure.

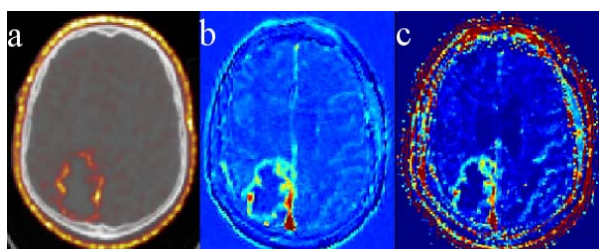


Figure. The figure show (a) SUV, (b) IAUGC60 and (c) Ktrans for the baseline exam of one patient included in the study.

Results: The correlation coefficient r was calculated for absolute values from baseline and 2 weeks, where no correlation was found to survival for any parameter. r was also calculated for relative change in parameters from 2 weeks to baseline, see table. Change in Ktrans mean, IAUGC60 mean and IAUGC60 max after two weeks was significantly correlated with survival. SUV(max) and the DCE-MRI parameters showed no significant correlations, see table.

No significant correlation of the SUV(max) and survival was found.

Table. The results of a correlation analysis of the variables to SUV(max) and survival after diagnosis. Statistically significant values ($\alpha = 0.05$) are highlighted in red, interesting but not significant results are highlighted in orange. Ktrans min was omitted due to division by zero when calculating the relative change.

Relative change in:	r	p	r	p
SUV(max)	SUV(max)	SUV(max)	Survival	Survival
SUV(max)	1	1	-0.055	0.895
Ktrans Mean	-0.602	0.152	0.724	0.042
Ktrans Max	-0.020	0.965	-0.184	0.662
Ktrans SD	-0.571	0.180	0.369	0.368
IAUGC60 Mean	-0.601	0.153	0.722	0.043
IAUGC60 Max	-0.595	0.158	0.774	0.024
IAUGC60 Min	-0.199	0.667	0.057	0.893
IAUGC60 SD	-0.685	0.089	0.657	0.076
Survival	-0.055	0.895	1	1

Conclusions: Our analysis indicates that the relative change in Ktrans mean, IAUGC60 mean and IAUGC60 max after two weeks correlates with survival after diagnosis. There was a large but not significant correlation between survival and IAUGC60 SD. The standard deviation in an ROI can be a crude marker for texture, something which has been shown as a promising tool for assessing treatment response and survival using e.g. 18F-FDG PET in esophageal cancer and ADC maps in gliomas. The results are promising, but a larger cohort is needed to confirm these initial findings.

PO-0959

Optimal dose balance between energy levels for material decomposition with dual-energy X-ray CT

G. Vilches-Freixas¹, J.M. Létang¹, K. Presich², P. Steininger², S. Rit¹

¹Université de Lyon CREATIS CNRS UMR5220 Inserm U1044 INSA-Lyon Université Lyon 1, Centre Léon Bérard France., Lyon, France

²Institute for Research and Development on Advanced Radiation Technologies, Paracelsus Medical University, Salzburg, Austria

Purpose/Objective: Dual-energy X-ray imaging is used to extract quantitative material information, e.g., electron density and effective atomic number Z , using the differences of X-ray attenuation coefficients of materials at different energies. A detailed study of factors that could influence the precision of extracted data is of importance. The aim of this study was to determine the optimal dose balance between the low and the high voltage acquisitions for material decomposition with dual-energy X-ray CT.

Materials and Methods: A model for the X-ray source spectra and the detector response of a prototype of the ImagingRing cone-beam CT (CBCT) scanner (MedPhoton, Salzburg, Austria) were built and validated experimentally using solutions from the literature. We then considered 30 cm-diameter homogeneous cylinder of selected materials. The analytical expression of the photon noise in CT images of [1] was adapted for polychromatic radiations. The energy-dependent